Fieldlike and Dampinglike Spin-Transfer Torque in Magnetic Multilayers

Claas Abert,[1,*] Hossein Sepehri-Amin,[2] Florian Bruckner,[1] Christoph Vogler,[3]
Masamitsu Hayashi,[2,4] and Dieter Suess[1]

[1]*Christian Doppler Laboratory of Advanced Magnetic Sensing and Materials, Faculty of Physics, University of Vienna, 1090 Vienna, Austria*
[2]*National Institute for Materials Science, Tsukuba 305-0047, Japan*
[3]*Institute of Solid State Physics, TU Wien, 1040 Vienna, Austria*
[4]*Department of Physics, The University of Tokyo, Bunkyo, Tokyo 113-0033, Japan*
(Received 1 December 2016; revised manuscript received 10 March 2017; published 12 May 2017)

We investigate the spin-transfer torque in a magnetic multilayer structure by means of a spin-diffusion model. The torque in the considered system, consisting of two magnetic layers separated by a conducting layer, is caused by a perpendicular-to-plane current. We compute the strength of the fieldlike and the dampinglike torque for different material parameters and geometries. Our studies suggest that the fieldlike torque highly depends on the exchange-coupling strength of the itinerant electrons with the magnetization both in the pinned and the free layer. While a low coupling leads to very high fieldlike torques, a high coupling leads to low or even negative fieldlike torques. Furthermore, we demonstrate the significant impact of the fieldlike torque on the critical switching current of a magnetic multilayer. Thus, the dependence of the fieldlike torque on material parameters is considered very important for the development of applications such as spin-transfer-torque magnetic random-access memories and spin-torque oscillators.

DOI: 10.1103/PhysRevApplied.7.054007

I. INTRODUCTION

Recently proposed magnetic storage technologies exploit the interaction of spin-polarized currents with the magnetization due to spin torque. Prominent examples for such devices are spin-transfer-torque magnetic random-access memories [1–3] and spin-torque oscillators that serve as field generators for microwave-assisted recording of hard-disk drives [4,5].

It is understood that the origin of spin torque is the interaction of spin-polarized conducting electrons with localized magnetic moments [6]. In semiclassical theories, such as micromagnetics, this polarization is represented by the spin accumulation $\boldsymbol{s}$ which describes the deviation of the spin carried by conducting electrons in the presence of charge current $\boldsymbol{j}_e > 0$ from the equilibrium situation at $\boldsymbol{j}_e = 0$. Magnetization dynamics under the influence of an effective field $\boldsymbol{h}_{\text{eff}}$ and spin accumulation $\boldsymbol{s}$ is governed by the Landau-Lifshitz-Gilbert equation

$$\frac{\partial \boldsymbol{m}}{\partial t} = -\gamma \boldsymbol{m} \times \left(\boldsymbol{h}_{\text{eff}} + \frac{J}{\hbar \gamma M_s} \boldsymbol{s} \right) + \alpha \boldsymbol{m} \times \frac{\partial \boldsymbol{m}}{\partial t}, \quad (1)$$

where $\boldsymbol{m}$ is the normalized magnetization, γ is the gyromagnetic ratio, α is the Gilbert damping, and J is the exchange strength between conducting electrons and magnetization.

A well-known system that exploits spin-torque effects is a three-layer structure consisting of two magnetic layers separated by a conducting nonmagnetic spacer layer. When applying a charge current perpendicular to the layers, one of the magnetic layers, referred to as the pinned layer, acts as a spin polarizer. When the spin-polarized electrons reach the second layer, referred to as the free layer, they accumulate at the interface and thereby exert a torque onto the free layer. The pinned layer generates a current with a spin polarization $\boldsymbol{M}$ parallel to its magnetization $\boldsymbol{m}_{\text{pinned}}$. Hence, it is natural to investigate the torque with respect to the polarization $\boldsymbol{M}$. The spin diffusion $\boldsymbol{s}$ can be written in a basis constructed by the magnetization $\boldsymbol{m}$ and a reference polarization $\boldsymbol{M}$

$$\boldsymbol{s} = a\boldsymbol{M} \times \boldsymbol{m} + b(\boldsymbol{m} \times \boldsymbol{M}) \times \boldsymbol{m} + c\boldsymbol{m}. \quad (2)$$

Inserting into (1) and considering $\|\boldsymbol{m}\| = 1$ yields

$$\frac{\partial \boldsymbol{m}}{\partial t} = -\gamma \boldsymbol{m} \times \left(\boldsymbol{h}_{\text{eff}} + \frac{Jb}{\hbar \gamma M_s} \boldsymbol{M} \right) - \boldsymbol{m} \times \left(\frac{Ja}{\hbar M_s} \boldsymbol{M} \times \boldsymbol{m} \right) + \alpha \boldsymbol{m} \times \frac{\partial \boldsymbol{m}}{\partial t}. \quad (3)$$

The torque term added to the effective field $\boldsymbol{h}_{\text{eff}}$ is usually referred to as fieldlike torque [7]. The second term is called spin-transfer torque or dampinglike torque, since it essentially leads to a relaxation of the magnetization $\boldsymbol{m}$ in the direction of the polarization $\boldsymbol{M}$. Accordingly, the coefficients a and b are proportional to the strength of the dampinglike and fieldlike torques, respectively.

*claas.abert@univie.ac.at

Despite its naming, the dampinglike torque does also contribute to the precessional motion of the magnetization. Also, the fieldlike torque leads to both precessional and dampinglike motion of the magnetization. This can be seen by transforming (3) into the explicit form of the Landau-Lifshitz-Gilbert equation that reads

$$\frac{\partial \boldsymbol{m}}{\partial t} = \frac{J}{\hbar M_s(1+\alpha^2)}[-(b+\alpha a)\boldsymbol{m}\times\boldsymbol{M} - (-a+\alpha b)\boldsymbol{m}\times(\boldsymbol{m}\times\boldsymbol{M})]. \quad (4)$$

In materials with low damping $\alpha \ll 1$, the fieldlike torque and the dampinglike torque, as previously defined, can be identified with precessional and dampinglike motion of the magnetization, respectively. However, in materials with high damping $\alpha \approx 1$ there is a strong intermixing of the fieldlike and dampinglike contributions.

A simple model for the description of spin torque in multilayer structures is the macrospin model by Slonczewski [8]. In this model, the coefficients a and b are defined in terms of the angle between polarization $\boldsymbol{M}$ and the magnetization in the free layer $\boldsymbol{m}$ as well as some general constants that depend on material parameters and the geometry of the system. However, the exact nature of this dependency is not provided by the model and thus the model constants are usually obtained by fitting simulation results to experimental data.

In this work, we use a drift-diffusion model to compute the spin accumulation $\boldsymbol{s}$ directly from material parameters and geometry. By projection onto the basis functions $\boldsymbol{M}\times\boldsymbol{m}$ and $(\boldsymbol{m}\times\boldsymbol{M})\times\boldsymbol{m}$ we obtain the spatially resolved coefficients a and b.

II. MODEL

Many models have been proposed in order to describe spin transport and spin torque in magnetic multilayers, among them Green's function [9,10] and different noncollinear generalizations of the work by Valet and Fert [11], see, e.g., Refs. [12–14]. In this work we use the drift-diffusion model introduced by Zhang, Levy, and Fert in Ref. [15] generalized to 3D [16]. The generalized Valet Fert models usually describe spin torque as an interface effect with the spin-mixing conductance being the constant of interest, which conflicts with experimental findings [17]. In contrast, the model used in this work describes the spin torque as a continuous effect whose penetration depth depends on the exchange coupling of the conducting electrons with the magnetization. In this model, the spin accumulation $\boldsymbol{s}$ is defined as

$$\frac{\partial \boldsymbol{s}}{\partial t} = -\boldsymbol{\nabla}\cdot\boldsymbol{j}_s - \frac{\boldsymbol{s}}{\tau_{\mathrm{sf}}} - J\frac{\boldsymbol{s}\times\boldsymbol{m}}{\hbar}, \quad (5)$$

where $\boldsymbol{j}_s$ is the spin current, τ_{sf} is the spin-flip relaxation time, and J is the same coupling constant as in Eq. (1). The spin current is given by

$$\boldsymbol{j}_s = \beta\frac{\mu_B}{e}\boldsymbol{m}\otimes\boldsymbol{j}_e - 2D_0\{\boldsymbol{\nabla s} - \beta\beta'\boldsymbol{m}\otimes[(\boldsymbol{\nabla s})^T\boldsymbol{m}]\}, \quad (6)$$

where β and β' are dimensionless polarization parameters and D_0 is the diffusion constant. Instead of the spin-flip relaxation time τ_{sf} and the coupling constant J, the material is often described in terms of the characteristic lengths $\lambda_{\mathrm{sf}} = \sqrt{2D_0\tau_{\mathrm{sf}}}$ and $\lambda_J = \sqrt{2D_0\hbar/J}$. While λ_{sf} is a measure for the decay of the spin accumulation due to spin-flip relaxation, λ_J is a measure for the penetration depth of the spin torque. Throughout this work we will use these material parameters that are more common in the experimental community. We numerically solve Eq. (5) assuming equilibrium $\partial\boldsymbol{s}/\partial t = 0$ with the finite-element method along the lines of Ref. [18]. Since the spin accumulation relaxes 2 orders of magnitude faster than the magnetization, this assumption has no significant influence on the magnetization dynamics. We apply homogeneous Neumann boundary conditions for $\boldsymbol{s}$ which corresponds to vanishing spin current at the boundaries, see Ref. [19]. In the experiments, the multilayer structure is usually contacted with nonmagnetic leads whose thicknesses are well above the decay length of the spin accumulation. In this case, no residual spin accumulation is expected at the outer interfaces of the leads which justifies the no-flux boundary conditions. However, for the numerical solution of Eq. (5) this would require a huge amount of finite elements to discretize the leads. In order to avoid computational overhead we use effective material parameters that allow us to model infinite leads with relatively thin nonmagnetic layers. This approach provides the exact same result for the spin accumulation within the magnetic regions as for infinite leads, see the Appendix.

In order to investigate the influence of material parameters and geometry onto the different torque terms, we consider the quasi-one-dimensional system depicted in Fig. 1. The system consists of two magnetic layers, a pinned layer (10 nm) and a free layer (5 nm). It is completed with a nonmagnetic spacer layer (5 nm) and two nonmagnetic leads (4 nm). For the magnetic layers, we choose material parameters similar to those of Heusler alloys, namely, $D_0 = 1\times10^{-3}\ \mathrm{m^2/s}$, $\beta = \beta' = 0.8$,

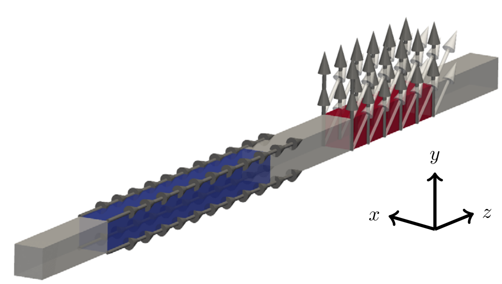

FIG. 1. The quasi-one-dimensional model. The fixed layer marked in blue is homogeneously magnetized in the z direction. The free layer marked in red is homogeneously magnetized in the yz plane. Two different configurations of the free layer are depicted.

$\lambda_{sf} = 8$ nm, and $\lambda_J = 1$ nm [20]. For the spacer we choose parameters similiar to Ag ($D_0 = 5 \times 10^{-3}$ m^2/s and $\lambda_{sf} = 100$ nm) and for the leads we choose parameters similar to Au ($D_0 = 5 \times 10^{-3}$ m^2/s and $\lambda_{sf} = 35$ nm) [21]. For homogeneous magnetization configurations, as considered in this work, the lateral dimension of the system does not have any impact on the solution of the spin accumulation and spin torque. Hence, we choose very small lateral dimensions (quasi–one dimensional) in order to speed up computations. Note, that in order to simulate infinite leads, we compute an effective diffusion length according to Eq. (A11), which leads to $\lambda_{sf}^{eff} \approx 11.6$ nm for a lead width of 4 nm.

III. RESULTS

The spin accumulation for the multilayer stack described in the preceding section is computed for a constant current $j_e = 10^{12}$ A/m^2 flowing perpendicular to the layers. Note that we compute the torques for a given magnetization configuration without considering the resulting dynamics of the magnetization. Since the spin accumulation, and thus also the torques, scale linearly with the current strength j_e, the choice of j_e does not have any influence on the qualitative results of this work. The current direction is chosen such that the conducting electrons pass the pinned layer before entering the free layer. The magnetization in the pinned layer (and thus also $\boldsymbol{M}$) is set homogeneously in the z direction, perpendicular to the layers. Unless specified differently, the magnetization in the free layer is set homogeneously in the y direction and the geometry as well as the material parameters are chosen according to the preceding section. The resulting spin accumulation $\boldsymbol{s}$ is projected onto $\boldsymbol{M} \times \boldsymbol{m}$ and $(\boldsymbol{m} \times \boldsymbol{M}) \times \boldsymbol{m}$, respectively, to obtain the strength of the dampinglike torque $T_{damp} = -Ja/\hbar\gamma M_s$ and the strength of the fieldlike torque $T_{field} = Jb/\hbar\gamma M_s$. Averaging over the free layer results in $\langle T_{damp} \rangle = 42\,444$ A/m and $\langle T_{field} \rangle = 2712$ A/m. These values are in good accordance with experimental findings [22]. The torques have a positive sign, i.e., the rotation caused by the fieldlike torque has the same direction as the rotation caused by an external field directed in the orientation of the pinned layer and the dampinglike torque is directed towards the orientation of the pinned layer. Moreover, the dampinglike torque is an order of magnitude larger than the fieldlike torque.

In a next experiment the influence of the exchange coupling of itinerant electrons and magnetization onto the different torque terms is investigated. Figure 2 shows the resulting $\langle T_{damp} \rangle$ and $\langle T_{field} \rangle$ for varying λ_J both in the free layer and the pinned layer. We choose λ_J as 0–4 nm, which is a realistic range according to Ref. [23]. The strength of the dampinglike torque does not significantly depend on the choice of λ_J, see Fig. 2(a). However, the fieldlike torque strength shows a very pronounced dependency. As shown in Fig. 2(b), not only the strength, but also the sign of the fieldlike torque may change depending on the choice of λ_J in the pinned and free layer.

For the magnetization configuration described above, namely homogeneous magnetization in the z direction in the pinned layer and homogeneous magnetization in the y direction in the free layer, the fieldlike torque strength T_{field} is, apart from a constant prefactor, given by the z component of the spin accumulation s_z. This component is plotted in Fig. 3 for varying characteristic lengths λ_J. The spin accumulation, and thus the fieldlike torque, is always positive at the interface between free layer and spacer layer. However, depending on λ_J in the free and pinned layer the spin accumulation performs a rotation, which may lead to negative values of s_z in parts of the free layer. Comparing Figs. 3(a) and 3(b) reveals that the influence of λ_J in the free layer has a significantly larger impact on this behavior. A high λ_J corresponds to a low J and thus a low spin coupling of the itinerant electrons with the magnetization. In this case, the behavior of the spin accumulation in the free layer is similar to the behavior in a nonmagnetic region, namely, the spin accumulation decays as $e^{-x/\lambda_{sf}}$. In the case of low λ_J, the spin accumulation experiences a torque due to the magnetization as the magnetization experiences a torque due to the spin accumulation. This torque explains the rotational behavior of the spin accumulation and thus also the possibility of negative values for s_z. Depending on the characteristics of this oscillation, the fieldlike torque becomes negative not only in parts of the free layer, but also in average. For strongly exchange-coupled systems this means that the overall fieldlike torque

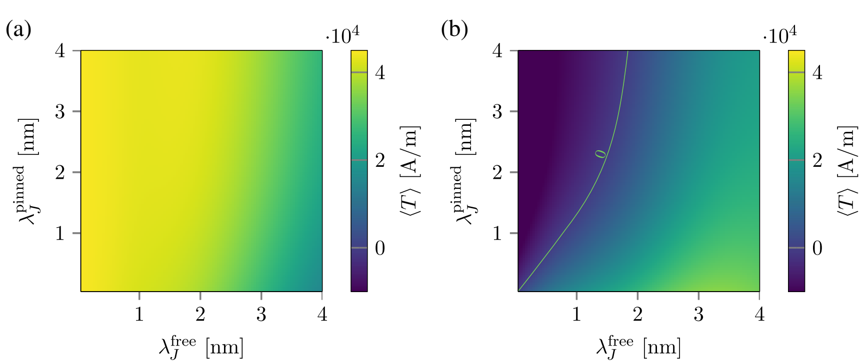

FIG. 2. Dampinglike and fieldlike torque for different exchange lengths in the pinned layer λ_J^{pinned} and the free layer λ_J^{free}. (a) Dampinglike torque T_{damp}. (b) Fieldlike torque T_{field}.

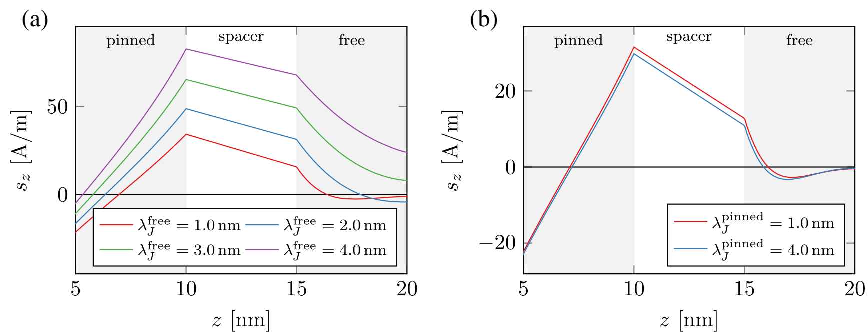

FIG. 3. Space-resolved z component of the spin accumulation s_z which is proportional to the fieldlike torque in the free layer. (a) $\lambda_J^{\mathrm{pinned}} = 1$ nm and different $\lambda_J^{\mathrm{free}}$. (b) $\lambda_J^{\mathrm{free}} = 1$ nm and different $\lambda_J^{\mathrm{pinned}}$.

in the free layer can have a negative sign. Not only the free layer but also the pinned layer exhibits a negative spin accumulation s_z at a large distance from the pinned layer-spacer interface. However, the reason for this is not the torque exerted onto the spin accumulation as in the case of the free layer, but the contribution of the lead-pinned layer interface that is not shown in Fig. 3. The z component of the spin accumulation of a homogeneously z magnetized layer enclosed by two nonmagnetic leads is negative at one interface and positive at the other depending on the sign of the electric current.

Besides the possible sign change of the fieldlike torque in the free layer, it should be noted that, depending on λ_J, the fieldlike torque may become as large as or even larger than the dampinglike torque. This is interesting since the fieldlike torque is usually assumed to be much smaller than the dampinglike torque and hence it is not considered to be relevant for applications. This behavior occurs at high λ_J in the free layer and low λ_J in the pinned layer, e.g., $\lambda_J^{\mathrm{free}} = 4$ nm and $\lambda_J^{\mathrm{pinned}} = 1$ nm results in $T_{\mathrm{damp}} = 19\,456$ A/m and $T_{\mathrm{field}} = 27\,933$ A/m.

Up to now, the free layer was considered to be magnetized in the y direction and thus perpendicular to the pinned layer. Figure 4 shows the averaged dampinglike and fieldlike torques for different tilting angles θ of the magnetization in the pinned layer and free layer. Here, $\theta = 0°$ means that the magnetization of the free layer points in the z direction like the pinned layer and $\theta = 90°$ means that the free-layer magnetization points in the y direction. The dampinglike torque shows the expected $\sin(\theta)$-like behavior with no notable dependence on $\lambda_J^{\mathrm{pinned}}$. However, the fieldlike torque shows a more complex dependence on the tilting angle θ. For large $\lambda_J^{\mathrm{pinned}}$ the fieldlike torque may even change its sign depending on θ.

In a final experiment, the interplay of the free-layer thickness d and the exchange length λ_J in the free layer is investigated. Figure 5 shows the dampinglike and fieldlike

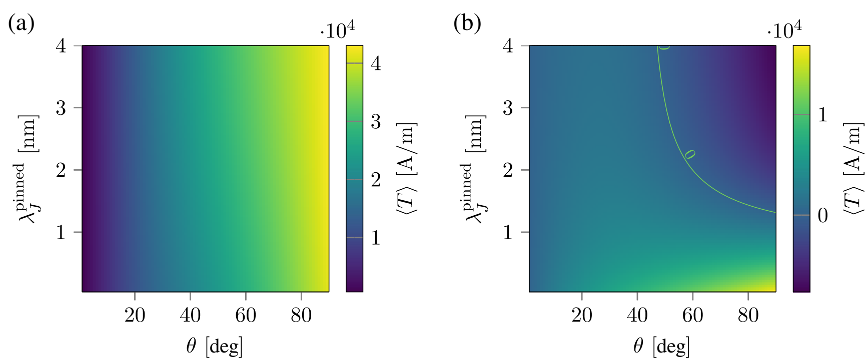

FIG. 4. Dampinglike and fieldlike torque for different exchange lengths in the pinned layer $\lambda_J^{\mathrm{pinned}}$ and tilting angle between magnetization in free and pinned layer θ. (a) Dampinglike torque T_{damp}. (b) Fieldlike torque T_{field}.

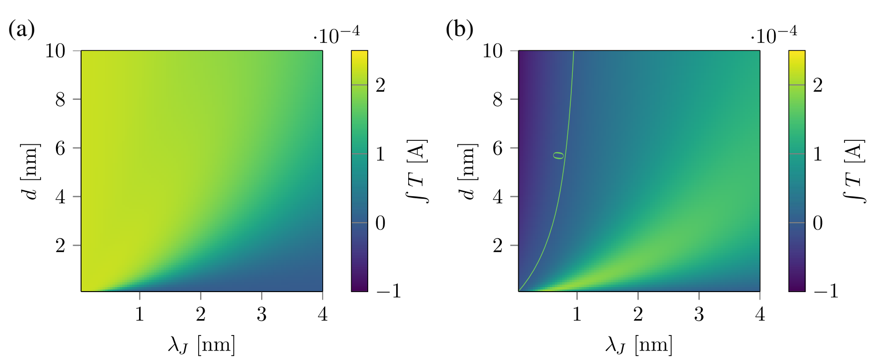

FIG. 5. Dampinglike and fieldlike torque for different thicknesses d and exchange lengths λ_J of the free layer. (a) Integrated dampinglike torque $\int T_{\mathrm{damp}} dx$. (b) Integrated fieldlike torque $\int T_{\mathrm{field}} dx$.

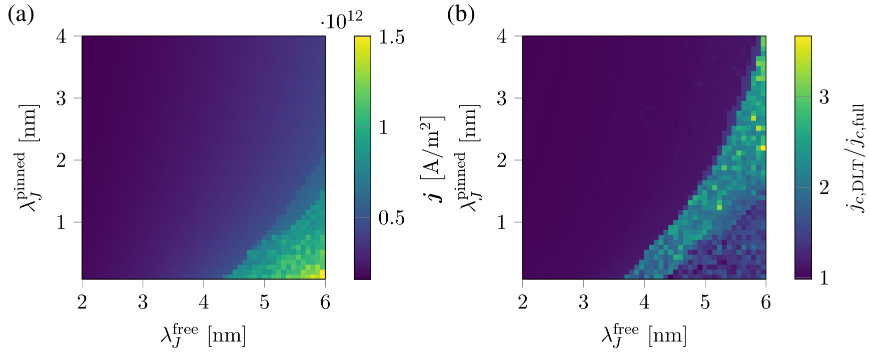

FIG. 6. Critical current for free-layer switching in magnetic multilayer. (a) Critical current for the full spin-diffusion model including fieldlike and dampinglike torque. (b) Ratio of critical switching current without fieldlike torque and with fieldlike torque $j_{c,\mathrm{DLT}}/j_{c,\mathrm{full}}$.

torque in the free layer. In contrast to the previous experiments, the torque is integrated and not averaged over the free layer in order to give a proper measure of the overall torque for the different layer thicknesses. The results can be explained with two different effects. For very small free-layer thicknesses, well below the characteristic length λ_J, the spin of the itinerant electrons is not completely transferred to the magnetization which results in a low overall torque. The critical thickness decreases for increasing λ_J which corresponds to low spin coupling. This effect can be clearly seen in both torque terms, Figs. 5(a) and 5(b). For the fieldlike torque, the rotation in the spin accumulation, as seen in the previous experiments, leads to low or even negative values for low λ_J. Figure 5(b) shows an approximately linear region of maximum fieldlike torque. It should be noted that the fieldlike torque is of the same order of magnitude as the dampinglike torque in the maximum region.

IV. MULTILAYER SWITCHING

Most spin-transfer-torque applications mainly exploit the dampinglike torque [24], both because it is usually considered much larger than the fieldlike torque in metallic junctions [24–26] and because it has a negligible impact on many processes due to its nature [27]. However, recent publications suggest that the fieldlike torque may have a significant impact on spin-torque oscillators [28,29] as well as on spin-transfer-torque magnetic random-access memories [30]. Here, we perform time-resolved simulations of the switching process in a magnetic multilayer in order to investigate the importance of the fieldlike torque. The system under consideration is the same as introduced in the preceding section. A perpendicular current is linearly increased with a rate of 10^{10} A/m^2 ns and the magnetization dynamics of the free layer are solved with a second-order backward-differentiation-formula scheme [31] according to Eq. (1). The free layer is considered to have perpendicular anisotropy with $K = 10^4$ J/m^3, a saturation magnetization of $M_s = 8 \times 10^5$ A/m^2, and a Gilbert damping of $\alpha = 0.01$. Furthermore, the exchange constant in the free layer is set to a very high value of $A = 10^{10}$ J/m in order to obtain a macrospinlike behavior and the pinned layer is tilted by $\theta = 5°$ in order to avoid a metastable state. The switching is simulated once with the full spin-diffusion model and once with the dampinglike contribution of the model only. In the second case, the full spin-diffusion model is solved and the fieldlike contribution to the torque is removed from the result.

Figure 6 shows the simulated critical current j_c for different λ_J in free and pinned layer. In regions of high $\lambda_J^{\mathrm{free}}$ and low $\lambda_J^{\mathrm{pinned}}$ the critical current is significantly lower for the full model compared to the model without fieldlike torque. Since this is exactly the region of high fieldlike torque, as shown in Fig. 2, we conclude that the switching process is strongly supported by the fieldlike torque.

Figure 7 shows the time evolution of the free-layer magnetization for $\lambda_J^{\mathrm{pinned}} = 1$ nm and $\lambda_J^{\mathrm{free}} = 5$ nm. The results for the full spin-diffusion model are compared to the results of the spin-diffusion model without fieldlike torque. The difference of the switching mechanisms in these two cases can be seen most clearly in the in-plane component of the magnetization m_x. While the in-plane magnetization performs strong oscillations in the case of the full simulation, these oscillations are pronounced less in the case of missing fieldlike torque. The in-plane oscillations are obviously caused by the fieldlike torque and have a large impact on the critical switching current for the investigated structure.

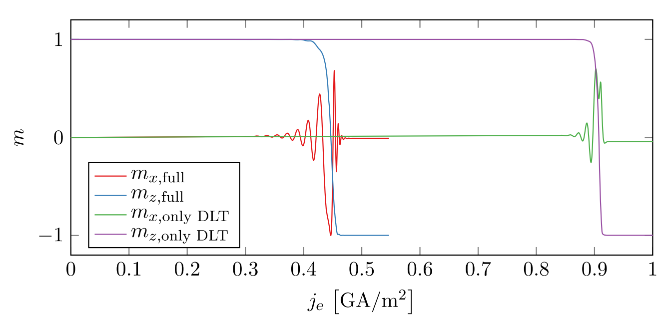

FIG. 7. Time evolution of free-layer magnetization during switching. The results for the complete solution of spin-diffusion model (full) are compared to the results of the model considering only the dampinglike torque (DLT).

V. CONCLUSION

The dampinglike and fieldlike torque in the free layer of a magnetic trilayer structure has been investigated with a spin-diffusion model. The exchange coupling of the itinerant electrons with the magnetization has been found to have a major impact on the strength and sign of the fieldlike torque. While the fieldlike torque is usually considered to be small compared with the dampinglike torque, we show that for a weak exchange coupling in the free layer, the fieldlike torque can excel the dampinglike torque. On the other hand, for a very strong coupling the sign of the fieldlike torque may change. In order to demonstrate the importance of the fieldlike torque strength, we compute the critical switching currents of a magnetic multilayer once with the full spin-diffusion model and once with the dampinglike torque only. The simulations suggest that a strong fieldlike torque is able to reduce the critical switching current significantly by a factor of 2 and more.

ACKNOWLEDGMENTS

The financial support by the Austrian Federal Ministry of Science, Research and Economy and the National Foundation for Research, Technology and Development as well as the Austrian Science Fund (FWF) under Grant No. F4112 SFB ViCoM, the Vienna Science and Technology Fund (WWTF) under Grant No. MA14-44, and MEXT Grants-in-Aid for Scientific Research (16H03853) of Japan is gratefully acknowledged.

APPENDIX: EFFECTIVE MATERIAL PARAMETER FOR FINITE LEADS

In the experiments, the size of the leads is usually much larger than the spin-diffusion length $\lambda_{\rm sdl}$ in the lead material. In order to retrieve accurate simulation results, the size of the leads has to be chosen accordingly, which adds a huge amount of additional degrees of freedom. However, by the choice of an appropriate effective spin-diffusion length, the effect of infinite decay can be perfectly modeled with finite leads. Without loss of generality, we consider the interface between the lead and magnetic region to be at $x = 0$, see Fig. 8. Assuming an infinite decay of the spin accumulation towards $-\infty$ yields

$$s(x) = a e^{x/\lambda_{\rm sf}}, \tag{A1}$$

where $\lambda_{\rm sf}$ is the spin-flip relaxation length, which equals the spin-diffusion length $\lambda_{\rm sdl}$ in metal, and a is constant determined by the solution of the model in the complete space. In order to simulate the infinite leads with finite leads, we introduce an effective spin accumulation $s_{\rm eff}$ that may contain decaying and ascending contributions

$$s_{\rm eff}(x) = a' e^{x/\lambda'_{\rm sf}} + b' e^{-x/\lambda'_{\rm sf}}. \tag{A2}$$

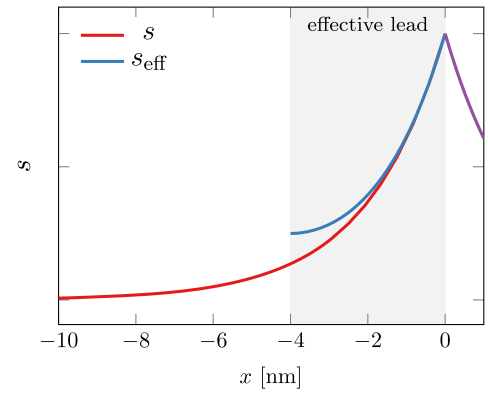

FIG. 8. Realistic spin accumulation s for infinite leads and effective spin accumulation $s_{\rm eff}$ for finite leads.

For the accurate solution of the spin accumulation in the magnetic material, both the spin accumulation $s_{\rm eff}$ and its first spatial derivative $s'_{\rm eff}$ have to be correct at the lead-magnet interface

$$s_{\rm eff}(0) = s(0), \tag{A3}$$

$$s'_{\rm eff}(0) = s'(0). \tag{A4}$$

We solve the spin-diffusion equation with homogeneous Neumann boundary conditions. Hence, additionally it holds

$$s'_{\rm eff}(-d) = 0, \tag{A5}$$

where d is the finite thickness of the lead. Inserting the definitions (A1) and (A2) yields the system

$$a' + b' = a, \tag{A6}$$

$$\frac{a'}{\lambda'_{\rm sf}} - \frac{b'}{\lambda'_{\rm sf}} = \frac{a}{\lambda_{\rm sf}}, \tag{A7}$$

$$\frac{a'}{\lambda'_{\rm sf}} e^{-d/\lambda'_{\rm sf}} - \frac{b'}{\lambda'_{\rm sf}} e^{d/\lambda'_{\rm sf}} = 0. \tag{A8}$$

From (A6) and (A7) we can derive

$$a' = \frac{a}{2}\left(1 + \frac{\lambda'_{\rm sf}}{\lambda_{\rm sf}}\right), \tag{A9}$$

$$b' = \frac{a}{2}\left(1 - \frac{\lambda'_{\rm sf}}{\lambda_{\rm sf}}\right). \tag{A10}$$

Inserting into (A8) yields

$$\left(1 + \frac{\lambda'_{\rm sf}}{\lambda_{\rm sf}}\right) e^{-d/\lambda'_{\rm sf}} - \left(1 - \frac{\lambda'_{\rm sf}}{\lambda_{\rm sf}}\right) e^{d/\lambda'_{\rm sf}} = 0. \tag{A11}$$

Given the real diffusion length of the infinite lead λ_{sf} and a finite lead thickness d, this system can be solved for the effective diffusion length λ'_{sf}. This procedure is precise and only suffers from discretization errors.

[1] Yiming Huai, Spin-transfer torque MRAM (STT-MRAM): Challenges and prospects, AAPPS Bull. **18**, 33 (2008).

[2] C. J. Lin, S. H. Kang, Y. J. Wang, K. Lee, X. Zhu, W. C. Chen, X. Li, W. N. Hsu, Y. C. Kao, M. T. Liu *et al.*, in *Proceedings of the 2009 IEEE International Electron Devices Meeting (IEDM)* (IEEE Publishing, Piscataway, 2009), pp. 1–4.

[3] A. V. Khvalkovskiy, D. Apalkov, S. Watts, R. Chepulskii, R. S. Beach, A. Ong, X. Tang, A. Driskill-Smith, W. H. Butler, P. B. Visscher *et al.*, Basic principles of STT-MRAM cell operation in memory arrays, J. Phys. D **46**, 074001 (2013).

[4] Jian-Gang Zhu, Xiaochun Zhu, and Yuhui Tang, Microwave assisted magnetic recording, IEEE Trans. Magn. **44**, 125 (2008).

[5] Jian-Gang Zhu and Yiming Wang, Microwave assisted magnetic recording utilizing perpendicular spin torque oscillator with switchable perpendicular electrodes, IEEE Trans. Magn. **46**, 751 (2010).

[6] Daniel C. Ralph and Mark D. Stiles, Spin transfer torques, J. Magn. Magn. Mater. **320**, 1190 (2008).

[7] A. A. Tulapurkar, Y. Suzuki, A. Fukushima, H. Kubota, H. Maehara, K. Tsunekawa, D. D. Djayaprawira, N. Watanabe, and S. Yuasa, Spin-torque diode effect in magnetic tunnel junctions, Nature (London) **438**, 339 (2005).

[8] John C. Slonczewski, Current-driven excitation of magnetic multilayers, J. Magn. Magn. Mater. **159**, L1 (1996).

[9] D. M. Edwards, F. Federici, J. Mathon, and A. Umerski, Self-consistent theory of current-induced switching of magnetization, Phys. Rev. B **71**, 054407 (2005).

[10] Christian Heiliger, Michael Czerner, Bogdan Yu. Yavorsky, Ingrid Mertig, and Mark D. Stiles, Implementation of a nonequilibrium greens function method to calculate spin-transfer torque, J. Appl. Phys. **103**, 07A709 (2008).

[11] T. Valet and A. Fert, Theory of the perpendicular magnetoresistance in magnetic multilayers, Phys. Rev. B **48**, 7099 (1993).

[12] Alexey A. Kovalev, Arne Brataas, and Gerrit E. W. Bauer, Spin transfer in diffusive ferromagnet–normal metal systems with spin-flip scattering, Phys. Rev. B **66**, 224424 (2002).

[13] J. Barnaś, A. Fert, M. Gmitra, I. Weymann, and V. K. Dugaev, From giant magnetoresistance to current-induced switching by spin transfer, Phys. Rev. B **72**, 024426 (2005).

[14] M. Gmitra and J. Barnaś, Current-Driven Destabilization of Both Collinear Configurations in Asymmetric Spin Valves, Phys. Rev. Lett. **96**, 207205 (2006).

[15] Shufeng Zhang, P. M. Levy, and A. Fert, Mechanisms of Spin-Polarized Current-Driven Magnetization Switching, Phys. Rev. Lett. **88**, 236601 (2002).

[16] Claas Abert, Michele Ruggeri, Florian Bruckner, Christoph Vogler, Gino Hrkac, Dirk Praetorius, and Dieter Suess, A three-dimensional spin-diffusion model for micromagnetics, Sci. Rep. **5**, 14855 (2015).

[17] A. Ghosh, S. Auffret, U. Ebels, and W. E. Bailey, Penetration Depth of Transverse Spin Current in Ultrathin Ferromagnets, Phys. Rev. Lett. **109**, 127202 (2012).

[18] Michele Ruggeri, Claas Abert, Gino Hrkac, Dieter Suess, and Dirk Praetorius, Coupling of dynamical micromagnetism and a stationary spin drift-diffusion equation: A step towards a fully self-consistent spintronics framework, Physica (Amsterdam) **486B**, 88 (2016).

[19] C. Abert, M. Ruggeri, F. Bruckner, C. Vogler, A. Manchon, D. Praetorius, and D. Suess, A self-consistent spin-diffusion model for micromagnetics, Sci. Rep. **6**, 16 (2016).

[20] T. M. Nakatani, T. Furubayashi, S. Kasai, H. Sukegawa, Y. K. Takahashi, S. Mitani, and K. Hono, Bulk and interfacial scatterings in current-perpendicular-to-plane giant magnetoresistance with Co_2Fe ($Al_{0.5}Si_{0.5}$) Heusler alloy layers and Ag spacer, Appl. Phys. Lett. **96**, 212501 (2010).

[21] Jack Bass, CPP magnetoresistance of magnetic multilayers: A critical review, J. Magn. Magn. Mater. **408**, 244 (2016).

[22] M. A. Zimmler, B. Özyilmaz, W. Chen, A. D. Kent, J. Z. Sun, M. J. Rooks, and R. H. Koch, Current-induced effective magnetic fields in Co/Cu/Co nanopillars, Phys. Rev. B **70**, 184438 (2004).

[23] Asya Shpiro, Peter M. Levy, and Shufeng Zhang, Self-consistent treatment of nonequilibrium spin torques in magnetic multilayers, Phys. Rev. B **67**, 104430 (2003).

[24] Nicolas Locatelli, Vincent Cros, and Julie Grollier, Spin-torque building blocks, Nat. Mater. **13**, 11 (2014).

[25] Jack C. Sankey, Yong-Tao Cui, Jonathan Z. Sun, John C. Slonczewski, Robert A. Buhrman, and Daniel C. Ralph, Measurement of the spin-transfer-torque vector in magnetic tunnel junctions, Nat. Phys. **4**, 67 (2008).

[26] Hitoshi Kubota, Akio Fukushima, Kay Yakushiji, Taro Nagahama, Shinji Yuasa, Koji Ando, Hiroki Maehara, Yoshinori Nagamine, Koji Tsunekawa, David D. Djayaprawira *et al.*, Quantitative measurement of voltage dependence of spin-transfer torque in MgO-based magnetic tunnel junctions, Nat. Phys. **4**, 37 (2008).

[27] Giulio Siracusano, Riccardo Tomasello, Massimiliano d'Aquino, Vito Puliafito, Anna Giordano, Bruno Azzerboni, Pat Braganca, Giovanni Finocchio, and Mario Carpentieri, Description of statistical switching in perpendicular STT-MRAM within an analytical and numerical micromagnetic framework, arXiv:1702.07739.

[28] M. Gmitra and J. Barnaś, Thermally Assisted Current-Driven Bistable Precessional Regimes in Asymmetric Spin Valves, Phys. Rev. Lett. **99**, 097205 (2007).

[29] Yuan-Yuan Guo, Hai-Bin Xue, and Zhe-Jie Liu, Oscillation characteristics of zero-field spin transfer oscillators with field-like torque, AIP Adv. **5**, 057114 (2015).

[30] R. K. Tiwari, M. H. Jhon, N. Ng, D. J. Srolovitz, and Chee Kwan Gan, Current-induced switching of magnetic tunnel junctions: Effects of field-like spin-transfer torque, pinned-layer magnetization orientation, and temperature, Appl. Phys. Lett. **104**, 022413 (2014).

[31] Dieter Suess, Vassilios Tsiantos, Thomas Schrefl, Josef Fidler, Werner Scholz, Hermann Forster, Rok Dittrich, and J. J. Miles, Time resolved micromagnetics using a preconditioned time integration method, J. Magn. Magn. Mater. **248**, 298 (2002).